Astronomy & Astrophysics manuscript no. Cabrera
(DOI: will be inserted by hand later)

February 2, 2008

Evidence for a deficit of young and old stars in the Milky Way inner in-plane disc

M. López-Corredoira[1], A. Cabrera-Lavers[2], O. E. Gerhard[1], F. Garzón[2,3]

[1] Astronomisches Institut der Universität Basel, Venusstrasse 7, CH-4102 Binningen, Switzerland
[2] Instituto de Astrofísica de Canarias, C/ Vía Láctea, s/n, E-38200 La Laguna, Tenerife, Spain
[3] Departamento de Astrofísica, Universidad de La Laguna, E-38200 La Laguna, Tenerife, Spain

Received xxxx / Accepted xxxx

Abstract. We give independent proof of the deficit of stars in the in-plane central disc ($2 < R < 4$ kpc, $|b| \lesssim 3^\circ$) with respect to the predictions of a pure exponential density distribution.
We use three different methods: 1) the inversion of the red clump giant distribution in near-infrared colour–magnitude diagrams to obtain the star density along the line of sight; 2) the determination of the density distribution of 1612 MHz sources by means of the distance determination of OH/IR sources from their kinematical information; 3) an analysis of near- and mid-infrared star counts and comparison with models. All the tests give the same result: a deficit of stars in the inner disc with respect to an exponential disc (either with constant scaleheight or extrapolated from the outer disc), but only in near plane regions ($|b| \lesssim 3^\circ$). This deficit might be interpreted as a flare in the vertical distribution. The in-plane density is almost independent of R and not an exponential law of the type $\rho \propto \exp(-R/h)$. Further away from the plane, however, the density increases towards the centre due to the increase of the scaleheight. Tests also show that this result cannot be due to extinction. This deficit affects both the young and the old populations, so it is probably a rather stable feature of the disc, and might be due to the existence of an in-plane bar sweeping the near-plane stars.
An approximate expression of the disc density within $2 < R < 8$ kpc is: $\rho(R,z) \propto e^{-\left(\frac{R}{1970\ \mathrm{pc}}+\frac{3740\ \mathrm{pc}}{R}\right)} e^{\frac{-|z|}{h_z(R)}}$, with $h_z(R) \approx 285[1 + 0.21\ \mathrm{kpc}^{-1}\ (R - R_\odot) + 0.056\ \mathrm{kpc}^{-2}\ (R - R_\odot)^2]$ pc.

Key words. Galaxy: general — Galaxy: stellar content — Galaxy: structure — Infrared: stars — radio: stars

1. Introduction

López-Corredoira et al. (2002, hereafter L02) obtained a model of the outer parts of the stellar disc (galactocentric radius R greater than 6 kpc), based on the 2MASS near infrared point sources survey. Among their findings are the stellar warp coincident with the gas warp, the flare, the absence of an external cut-off out to $R = 15$ kpc and the measurement of the different parameters of the old population density distribution, generally in agreement with other independent studies. Here, we continue the analysis of the disc structure in the inner stellar disc, examining whether or not this corresponds to an extrapolation of the L02 disc model towards the centre and, if not, what the differences are.

A major concern is whether extrapolation of the exponential in the inner stellar disc is appropriate or whether there is some deficit of stars with respect to this distribution. It is well known that many barred galaxies have holes (Ohta et al. 1990); up to half of them, according to Anderson et al. (2002) based on analysis of the bulge-disc decomposition carried out in Baggett et al. (1998). In a large number of external galaxies, due to their more favourable orientation, the central hole in the disc has been detected in the distribution of molecular and atomic gas. See, for example, Aguerri et al. (2001), who describe a hole in the HI distribution in NGC 5850 associated with the central bar region, as is the case presented by Bottema & Verheijen (2002) in NGC 3992. These holes have been attributed to the presence of gas velocities perpendicular to the Galactic plane (Sancisi 1999). However, there are also cases where the CO distribution, used to infer the HII density, does not reveal such a hole, as is the case, for example, of Sakamoto et al. (1999), whose sample is somewhat biased towards the non-hole gas distribution because of selection criteria. The hole does not usually consist strictly of an abrupt truncation of the disc. It can represent a gradual density decrease (for instance, Freeman type II truncation; Freeman 1970), instead of increasing towards the center within a certain radius, or even a constant density or increasing density but with a slope much

Send offprint requests to: acabrera@ll.iac.es

lower than that produced by the extrapolated exponential law.

In our Galaxy, this hole (from now on, we will call the hole a "deficit" of gas or stars since, strictly speaking, the hole is not totally empty; "deficit" here is always with respect to the extrapolation of the purely exponential disc towards the inner radii) is observed in the gas distribution (i.e., Robinson et al. 1988). For the stellar distribution the answer is not very clear at present. Several disc models have been produced using COBE/DIRBE flux maps. Although the general features are approximately coincident, it seems that there is no agreement regarding the deficit of stars. For instance, Freudenreich (1998) and Lépine & Leroy (2000) agree that there is a such a deficit, while Bissantz & Gerhard (2002, hereafter B02) can reproduce quite accurately the flux maps with an exponential disc even in the inner parts. Caldwell & Ostriker (1981) gave a model of the disc that consists of a difference of two exponentials with different scalelengths, which gives a deficit of stars in the inner part (see fig. 15 in Caldwell & Ostriker 1981) based on kinematical measurements. Microlensing experiments seemed to favour a deficit of stars (Kiraga & Paczyński 1994), but the poorly–known interstellar extinction at optical wavelengths gives some uncertainties in their models. Moreover, Kiraga et al. (1997) recognize that their previous paper might contain some errors due to an incorrect identification of populations in the optical colour–magnitude diagrams. Analysis of OH/IR sources, both from the young and intermediate–old populations, led Baud et al. (1981) to conclude that there must be a deficit of stars in the two populations; these results are more convincing, and we think that a corroboration of this result with newer surveys will be valuable (see §5). This topic has so far not received much attention in terms of star counts. López-Corredoira et al. (2001, hereafter L01) have claimed that a deficit of stars is necessary to reproduce some near-plane counts but they did not try to fit off-plane regions, and not too much attention was paid to the problem in that paper. Precisely because of this, we wish to examine the possible deficit of stars in the inner disc, using point source catalogues, which contain more information than flux-maps alone.

A further area of study is the real nature of the deficit of stars, should this be genuine. A flared stellar distribution places the stars at a higher elevation from the plane than that predicted from a pure exponential law, hence giving the impression of a hole in the plane. Flared structures are well recognized in the distribution of gas (see Burton & Hekkert 1986) and stars (L02; Alard 2000, and references therein) in the outer disc. The presence of that type of morphology in the central disks of spiral galaxies is not so well studied due to the inherent difficulties in separating the several structural contributions to the observed counts or flux. A good example of that difficulty can be found in Nikolaev et al. (2004), who reported a symmetric warp in the inner disk, the central 4 degrees, of the LMC based on accurate analysis of MACHO and 2MASS counts.

2. Data

The data for this work were taken from several sources: mainly 2MASS, MSX and ATCA/VLA, and some other DENIS and TMGS data taken from a former paper (L01). The second release of the 2MASS project (Skrutskie et al. 1997, http://www.ipac.caltech.edu/2mass/releases/docs.html) provides us with some data in the regions of interest to study the inner disc isolated from other components ($1.5^\circ < |b| < 6.5^\circ$, $15^\circ < l < 40^\circ$). We use these data to produce K-band star counts (m_K) and m_K vs. $(J-K)$ colour–magnitude diagrams (CMDs) in the regions given in Table 1. The MSX Point Source Catalogs (version 1.2; Egan et al. 1999) provides us with star counts in the D (14.65 μm) mid-infrared band in the regions $|b| < 0.5^\circ$, $|l| < 45^\circ$. OH/IR stars from the ATCA/VLA catalogue (Sevenster et al. 1997a,b, 2001) in the radio maser line at 1612.23 MHz at $|b| < 2.5^\circ$, $|l| < 45^\circ$ were used to obtain star counts and the distribution of the sources as a function of galactocentric radius.

Table 1. Selected regions used to extract the colour–magnitude diagram from 2MASS sources so as Ato apply the method of §3

l (deg)	b (deg)	area (deg^2)
15	2	0.57
15	3	1.00
15	−3	1.00
15	−6	1.00
18	−2	0.92
18	−3	0.97
20	−3	1.00
20	−6	1.00

3. The inner disc from CMD analysis

3.1. Method

In L02 (§3), some of us developed a method to obtain the star density along a line of sight (l, b) from an analysis of near-infrared CMDs, such as m_K vs. $(J-K)$, which are the colours to be used here. First, the trace produced in the CMD by the red clump giants (spectral type: K2 III) is identified. This is easy because they are much more abundant than the other giants (Cohen et al. 2000; Hammersley et al. 2000). Second, we count the number of stars within a 0.4 mag width trace as a function of the apparent magnitude (examples are given in L02 and in Figs 1, 2 of this paper). Third, because we know their absolute magnitude and intrinsic colour [$M_K = -1.65$, $(J-K)_0 = 0.75$; L02], we can obtain the extinction and density as a function of distance along the line of sight. The correction of the mean extinction is carried out since we can measure the reddening of the K2 III stars. The details are explained in L02(§3), so they will not be repeated here.

Recent results in open clusters also give similar results for the intrinsic luminosity of the red clump (Grocholski & Sarajedini 2002): magnitude −1.62 with a standard deviation of 0.21 and colour $(J-K)_0$ around 0.7 for the age of the old disc population with a small dispersion due to metallicity or age gradients. Pietrzyński et al. (2003) also show that the K-band magnitude of red clump is a good distance indicator, and that the colour has only a very slight dependence on the metallicity. Theoretical predictions from isochrones (Salaris & Girardi 2002) agree with these values. Therefore, counts can give us information about the extinction along the line of sight as well as the density of K2 III stars: $\rho_{\rm K2\,III}(r,l,b)$, which leads to $\rho_{\rm K2\,III}(R,z)$, assuming axisymmetry in the disc (r = distance from the Sun, R = distance from the centre of the Galaxy).

Concerning the completeness in crowded fields, in the worst cases ($l = 15°$, $b = 2°$) the survey is complete to magnitudes $m_K \approx 13.2$ and $m_J \approx 14.4$. The reddening due to the extinction is less than $\Delta(J-K) = 0.75$. Since we use the red clumps with $(J-K)_0$ between 0.55 and 0.95 (the width of the strip is 0.4 mag), we will adopt a limit of $m_K < 12.7$ (instead of 13.0 used in L02) to be sure of the completeness of the sources.

Poisson errors will be important for very bright stars (i.e. close stars, since the absolute magnitude is constant). If we look towards the centre of the Galaxy, the Poisson error will be important for distances from the Sun $r < 3$ kpc (galactocentric distance $R \gtrsim 5$ kpc), but it will be reasonably small for $R = 2$–5 kpc, where the inner disc can be examined. The method works reasonably well for r greater than ~ 3 kpc, and this was tested with real data by L02, who demonstrated that the parameters of the outer disc obtained by this method are consistent with those obtained by other methods. The global systematic errors of this method are less than 10% for the regions with low extinction in a typical anticentre direction (L02). In the present paper, the areas are somewhat more extinguished (up to 0.45 mag in K instead of 0.2 mag in L02, total extinction out to 7–8 kpc along the line of sight) and the regions are towards the centre of the Galaxy instead of the outer disc regions used in L02, which might give a somewhat higher contamination of M-giants. This, however, will give systematic errors of the same order, as will be shown below, perhaps only slightly larger, and the method is therefore appropriate for measuring the density of the inner disc stars.

3.1.1. A simulation to test the method

To show how well the method works, we will carry out a Monte Carlo simulation. We will generate a synthetic colour–magnitude diagram with a population model and a predescribed density model. From this CMD, we will obtain the density along the line of sight using the method of extracting the clump giants, and this will be compared with the original density.

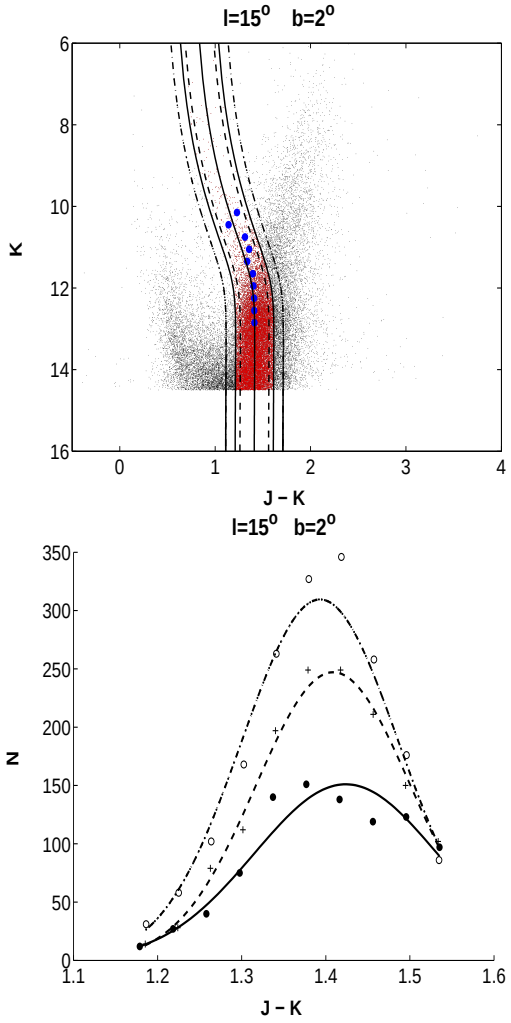

Fig. 1. Top: Colour–magnitude diagram for the line of sight $l = 15°$, $b = 2°$ used in the present section with 2MASS data. The solid line shows the fitted trace that we assign to the red clump giant population and the limits for the red clump giants within a width of 0.4 mag. Dashed lines show the limits for a width of 0.3 mag. Dot–dashed line show the limits for a width of 0.6 mag. Bottom: histograms of counts (per unit colour) for three fixed apparent magnitudes and the corresponding best Gaussian fits: m_K=11.95 (dots/solid line), m_K=12.25 (crosses/dashed line), $m_K = 12.55$ circles/dot–dashed line. $\Delta m = 0.3$.

The information about the absolute magnitudes and relative abundances of all possible stellar spectral types was taken from the updated SKY model (Wainscoat et al. 1992; M. Cohen, private communication). The red clump with the range of intrinsic colours of 0.2 mag and range of absolute magnitudes of 0.3 mag (L02) is represented by the K0–5 III population with a peak in K2–3 III; this population represents the clump with mean absolute magnitude −1.65 and color $(J-K)_0 = 0.75$, with Gaussian dispersions with the referred sigmas. Poisson noise in the density is also introduced in the simulation.

Since the region at $l = 15°$, $b = 2°$ has a higher contamination of M-giants (because the ratio of dis-

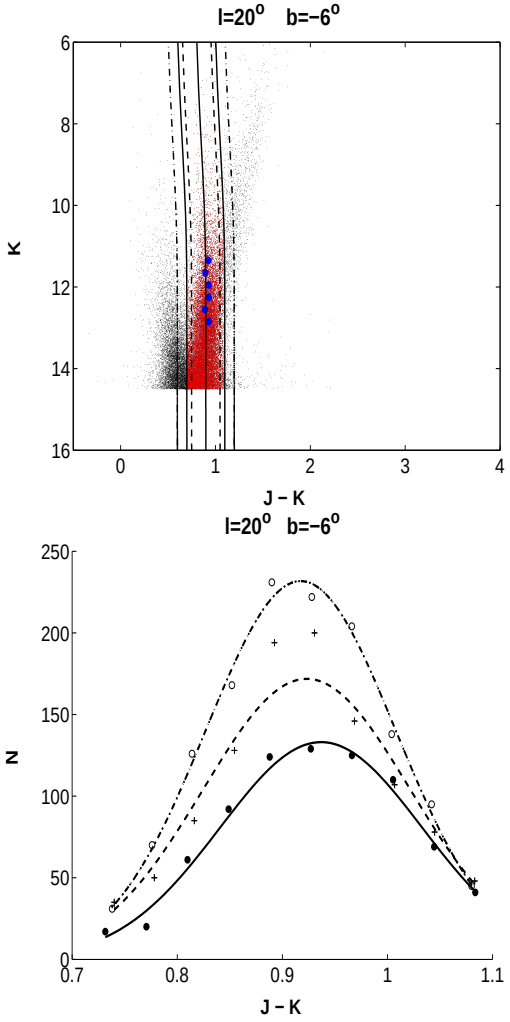

Fig. 2. Top: Colour–magnitude diagram for the line of sight $l = 20°$, $b = -6°$ used in the present section with 2MASS data. The solid line shows the fitted trace that we assign to the red clump giant population and the limits for the red clump giants within a width of 0.4 mag. Dashed lines show the limits for a width of 0.3 mag. Dot–dashed line show the limits for a width of 0.6 mag. Bottom: histograms of counts (per unit colour) for three fixed apparent magnitudes and the corresponding best Gaussian fits: $m_K = 11.95$ (dots/solid line), $m_K = 12.25$ (crosses/dashed line), m_K=12.55 circles/dot–dashed line. $\Delta m = 0.3$.

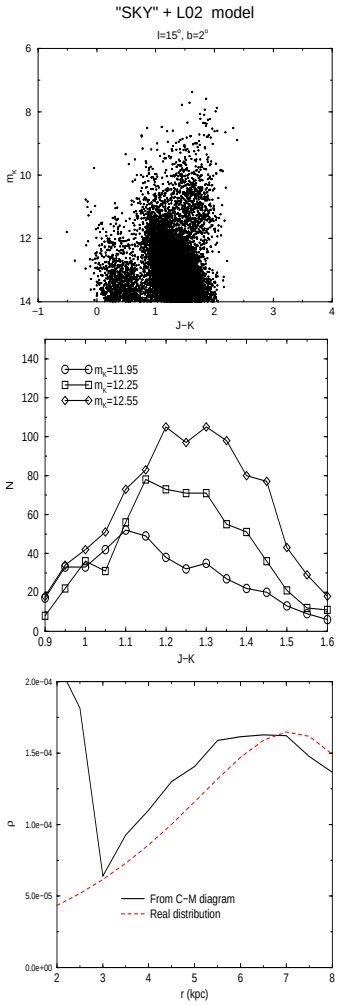

Fig. 3. Top: Synthetic colour–magnitude diagram derived from the SKY model for the populations and relative abundance and an exponential disc (larger density for low values of R). Centre: histograms of counts for fixed m_K ($\Delta m_K = 0.3$). Bottom: density along the line of sight in the field $l = 15°$, $b = 2°$: comparison between the "real" assumed density and the corresponding densities obtained from the CMD analysis method with width = 0.4 mag of the synthetic colour–magnitude diagram.

tant/nearby stars is larger) and the highest extinction, we will carry out our experiments in this line of sight. This is the one with the largest errors, so the other lines of sight will have lower errors than the present one. We carry out two experiments: 1) with a pure exponential disc: $\rho(R,z) \propto e^{-R/H} e^{-|z|/h_z}$ ($R_\odot = 7.9$ kpc, scalelength $H = 0.25 R_\odot$, scaleheight $h_z = 0.036 R_\odot$; L02); 2) for a model with the same density for $R > 4$ kpc, but $\rho(R,z) \propto e^{-|z|/h_z}$ (i.e. independent of galactocentric distance) for $R \leq 4$ kpc. The results are shown in Figs 3 and 4.

The colour–magnitude diagrams in Figs 3 and 4 approximately reproduce the one observed in Fig. 1. They are not perfectly equal, but it is not our purpose to discuss the validity of the SKY model here. Our purpose is to test the density extracted through the clump giant extraction method. This is tested in the right-hand part of Figs 3 and 4 (for $r > 3$ kpc; for lower distances, the Poisson error and the M-giant contamination dominate, but we are not interested in this range). In both cases, the density is approximately that of the model. There are excesses of 20–30% between $r = 4$–6 kpc due the contamination of the M-giants. The density distributions in both cases can be clearly distinguished and the method is able to detect the differences of the density in Figs 3 and 4. This is the worst case among the selected lines of sight. Statistically (when we use the data of all the lines of sight), the errors

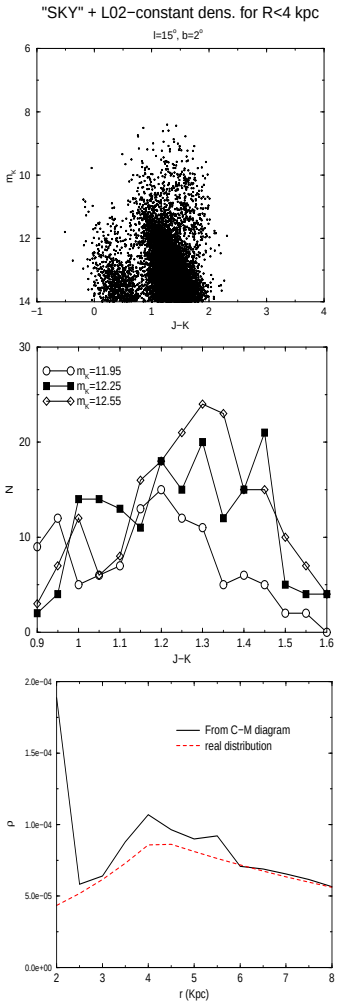

Fig. 4. Top: Synthetic colour–magnitude diagram derived from the SKY model for the populations and relative abundance, and an exponential disc for $R > 4$ kpc and constant density (independent of R) for $R < 4$ kpc. Centre: histograms of counts for fixed m_K ($\Delta m_K = 0.3$). Bottom: density along the line of sight in the field $l = 15°$, $b = 2°$: comparison between the "real" assumed density and the corresponding densities obtained from the CMD analysis method with width = 0.4 mag of the synthetic colour–magnitude diagram.

are lower: roughly 10–15% for $r = 4$–6 kpc and even less beyond.

3.1.2. Uncertainties due to the patchiness of extinction

The extinction is corrected on average because we know the reddening. In extracting the red clumps from the colour–magnitude diagram, we ask whether the patchiness of the extinction, i.e. the fluctuations in A_K relative to the mean extinction, could have some effect (characterized by dispersion σ_{A_K}). This is an additional effect to consider which was not discussed in §3.1.1. It would produce an extra dispersion in the apparent magnitudes (which, if less than ~ 0.3 mag, produces negligible errors in an exponential distribution; see L02, §3.3.1) and an extra dispersion in the reddening, which can result in the loss of some stars because they move to a position in the CM diagram that is outside the selected trace of red clump giants with width 0.4 mag (see L02, §3). Since the intrinsic dispersion of colours is around 0.2 mag, the extra dispersion with respect to the central position of the trace would be (for $\Delta(J-K) = 1.52 A_K$; Rieke & Lebovsky 1985):

$$\sigma_{(J-K),\mathrm{centre\ trace}} = 1.52\sigma_{A_K} - \frac{\sigma_{A_K}}{\left(\frac{dm_K}{d(J-K)}\right)}, \quad (1)$$

where the first term is the absolute value of the reddening and the second term is the $(J-K)$ variation of the centre of the trace corresponding to this extra extinction. $\frac{dm_K}{d(J-K)}$ is the equation of the centre of the trace. From the relation between apparent magnitude and the extinction, we get

$$\frac{dm_K}{d(J-K)} = \frac{\frac{dm_K}{dr}}{\frac{d(J-K)}{dr}} = \frac{\frac{5\log_{10} e}{r} + \frac{dA_K}{dr}}{1.52\frac{dA_K}{dr}} = 0.658 + \frac{1.43}{r\frac{dA_K(r)}{dr}} \quad (2)$$

Consequently, for instance for $r = 5$ kpc at $l = 15°$, $b = 2°$ (corresponding to $R = 3.4$ kpc): $\sigma_{(J-K),\mathrm{centre\ trace}} = 1.13\sigma_{A_K}$. For larger values of r (lower R) the effect is somewhat lower because the second term of eq. (1) becomes more important: for instance, $\sigma_{(J-K),\mathrm{centre\ trace}} = 0.92\sigma_{A_K}$ (for $r = 7$ kpc). This extra broadening of the distribution will lead to a loss of stars for a fixed width of the trace. Assuming that this extra broadening and the intrinsic broadening of the distribution are Gaussian, the ratio of lost stars would be that plotted in Fig. 5 for $l = 15°$, $b = 2°$.

A Monte Carlo simulation was also carried for the cases of Figs 3 and 4 but adding the effect of patchiness of extinction. Fig. 6 shows the result. The effect of the patchiness of extinction might be important, but only in cases with $\sigma_{A_K} = 0.6 A_K$ or larger, while the expected cases are under $0.2 A_K$, as will be shown now.

To determine whether the patchiness of extinction is significant it is necessary to evaluate the dispersion of this extinction. An examination of the Schultheis et al. (1999) and L01 maps of extinction (with a resolution of 2 arcminutes) for $|l| < 20°$, $|b| < 2°$ in A_V gives a spread (due to both patchiness and gradient) of around 20% with respect to the mean extinction, almost independently of which region in the centre of the Galaxy is considered.

Lada et al. (1999) have shown that the variations in extinction through the dark cloud IC 5146 for each background star due to small-scale fluctuations (once the large–scale gradients are removed, i.e. taking small regions) are less than 18% of the mean extinction. If this is correct for the Milky Way extinction in general, it would indicate that the patchiness is limited within the value of $\sigma_{A_K} = 0.20 A_K$, or even less if we integrate along a line of sight that passes through several clouds, as would be the case for near-plane regions.

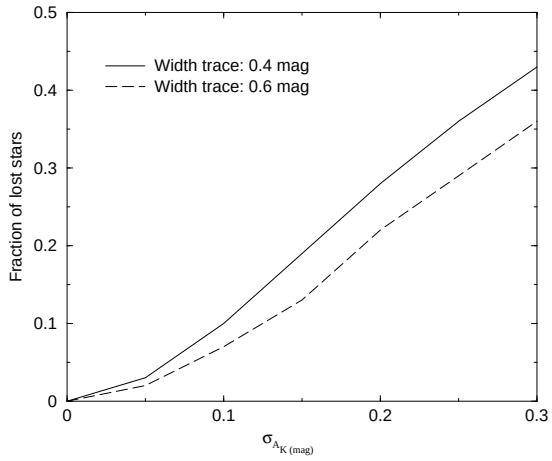

Fig. 5. Fraction of lost stars due to the spread of the extinction in the field $l = 15°$, $b = 2°$ for $r = 5$ kpc. Two values for the width of the K2 III strip are used. In the subsequent analysis, a width of 0.4 mag is used.

Since our region has 0.5 mag of mean extinction, this would give $\sigma_{A_K} \approx 0.10$ mag, i.e. a loss of 10% of the stars in our case (7% for width 0.6 mag). This would be nearly the same for any r between 5 and 6.5 kpc (R between 2.3 and 3.5 kpc). This is the worst of the cases, because the rest of the lines of sight are less extinguished and are consequently less patchy. A model with a substantial deficit of stars (such as the one we will obtain below) gives an absence of 60–70% of stars with respect to the purely exponential L02 model at this latitude. A σ_{A_K} value of around 0.40 mag, four times our estimate, would be necessary to explain this, which makes this method able to detect a deficit of stars of this order.

The effect of the gradient of extinction may be shown to be insignificant overall. For the most extinguished region ($l = 15°$, $b = 2°$), the effect of the gradient of extinction due to variation of b between 1.5° and 2.5° is $\frac{\sigma_{A_K}}{A_K} = \frac{\Delta b}{2\sqrt{3}} \frac{d(ln\ A_K)}{db}$ and $\frac{d(ln\ A_K)}{db} \approx 0.49$ (Wainscoat et al. 1992); the gradient in extinction in the latitude direction produces a dispersion of $\sigma_{A_K} \approx 0.07$ mag, which is certainly not Gaussian but for a rough estimate can be considered so. From Fig. 5, we will see that this can produce a 5–7% loss of stars, which may be considered unimportant.

3.2. Application of the method

We selected eight regions (see Table 1) in $|l| = 15$–$20°$. In this zone, the disc is far enough from the bulge that the contribution of bulge stars in the extracted red clump giant strip is small, and it is close enough to the Galactic Centre to have lines of sight reaching $R = 2$–4 kpc, where the inner disc will be studied.

Different latitudes were selected so as to have a representation of different heights, except in plane regions, where the extinction might be excessive and/or very irregular in spatial distribution, and the hypothetical in-plane bar would presumably contaminate the counts (L01).

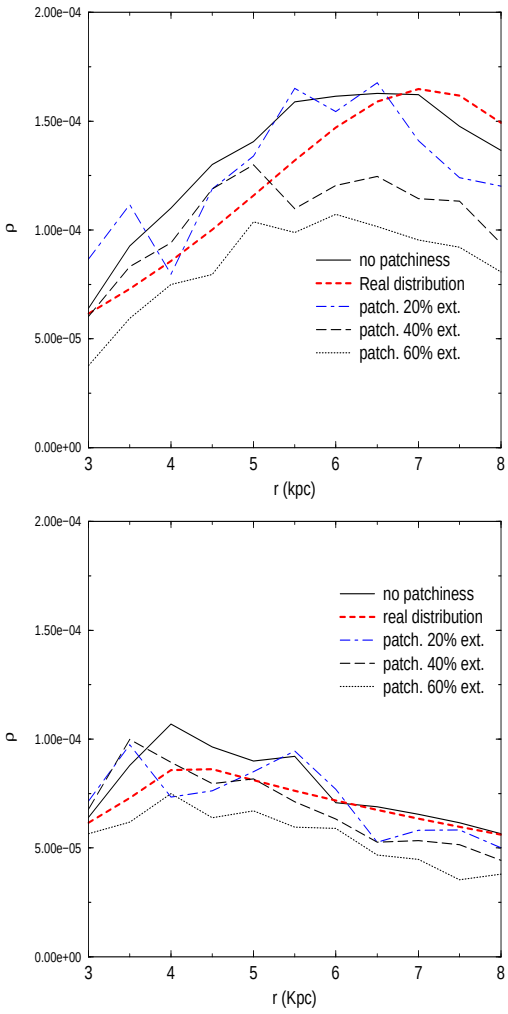

Fig. 6. Density along the line of sight in the field $l = 15°$, $b = 2°$ [a) exponential disc as in Fig. 3; b) with constant density for $R < 4$ kpc as in Fig. 4]: comparison between the inputs of the density and the density distribution obtained from the CMD analysis method with width = 0.4 mag of the colour–magnitude diagram generated by a Monte Carlo simulation. Models with four different patchiness are plotted: $\sigma_{A_K} = 0, 0.2A_K, 0.4A_K, 0.6A_K$.

The density $\rho_{\mathrm{K2\,III}}(R, z)$ along the eight lines of sight was obtained (see Figs 7). An extrapolation of the exponential L02 model does not fit these data: the model gives only ∼30% of the density at $b = -6°$, which means that the extrapolation of the flare (the decrease in h_z with decreasing R) found in L02 for the external disc is not appropriate for the inner disc. If we extrapolate the exponential L02 disc but without a flare, the result is better for $b = -6°$, but there is an excess of ∼200% in the density at $|b| = 2°$. It is clear that an exponential disc does not work either with or without a flare of increasing h_z for increasing R, according to the extrapolation of L02, or with any intermediate option.

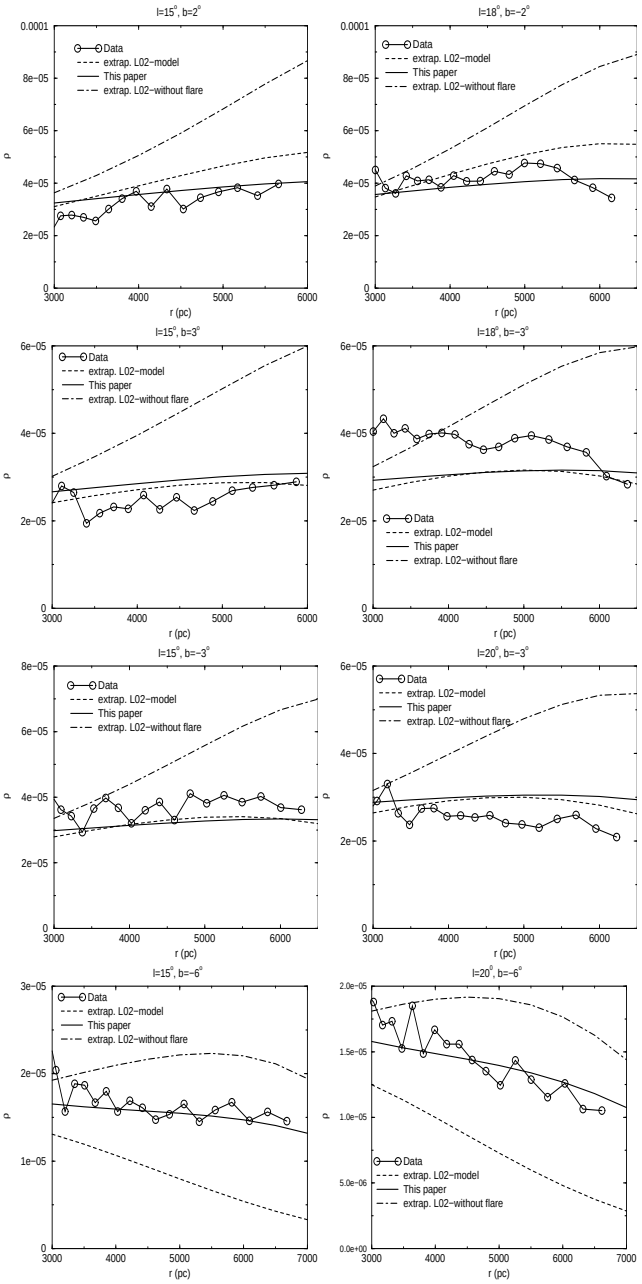

Fig. 7. Density along the different lines of sight. An extrapolation of the exponential L02 model does not fit these data: the model gives only ∼30% of the density at $b = -6°$, which means that the extrapolation of the flare (the decrease in h_z with decreasing R) found in L02 for the external disc is not appropriate for the inner disc. To fit these data, a density nearly independent of R must be introduced (thicker solid line in the plot), which will be obtained in this paper [eqs. (3) and (6)].

In Fig. 8, the densities are plotted as a function of z for different R in $R < 4$ kpc (note that, for the calculation of $z(r, l, b)$, we take into account that the Sun is 15 pc above the plane, but not the effects of the warp described in L02 since they are negligible for the inner disc; the warp is important for regions near $|l| = 90°$ and $R > 10$ kpc). In these plots, we observe how the scaleheight changes with R; it increases towards the centre: $h_z(2.5\ \mathrm{kpc}) = 424 \pm 46$ pc, $h_z(3\ \mathrm{kpc}) = 352 \pm 23$ pc, $h_z(3.5\ \mathrm{kpc}) = 338 \pm 48$ pc, $h_z(4\ \mathrm{kpc}) = 323 \pm 26$ pc. A weighted fit of a linear law of h_z gives:

$$h_z = 317 \pm 17 - [R(\mathrm{kpc}) - 4]48 \pm 20\ \mathrm{pc}, \quad (3)$$

for 2.25 kpc < R < 4.25 kpc. Therefore, we have a higher scaleheight in the inner disc with the opposite trend to that of the outer disc, which, according to L02, ranges from 230 and 285 pc between $R = 6$ kpc and $R_\odot$: here, h_z slightly decreases with increasing R. Eq. (3) is valid for $R < 4.25$ kpc while that given by L02 is valid for $R > 6$ kpc. In the range between 4 and 6 kpc the scaleheight dependence on radius is somewhat uncertain but is presumably the region where h_z is at a minimum.

One might suspect the contamination of the bulge to be responsible for this increase in the scaleheight. However, the bulge contribution is negligible. Using the bulge model of axial ratios 1:0.54:0.33 of López-Corredoira et al. (2000), we find that the largest bulge/disc ratio is for $l = 15°$, $b = -6°$, $R = 2245$ pc which gives a contribution $\rho_{\mathrm{bulge}} = 5 \times 10^{-3}$ pc^{-3}. Since the K2 giants are $\approx 10^{-4}$ times the total number of stars (L02), this gives $\rho_{\mathrm{K2\,III,bulge}} \approx 5 \times 10^{-7}$ pc^{-3} = 5% of the total K2 III density, which is less than the other errors. Higher ellipticity models of the triaxial bulge (such as that of B02) would give even less bulge contamination. This is the most favourable line of sight for the bulge; for the other (l, b, R) the bulge contamination is even lower.

Once we know the scaleheight as a function of the radius, $h_z(R)$, we can calculate

$$\rho_{\mathrm{K2\,III}}(R, z = 0) \equiv \frac{\rho_{\mathrm{K2\,III}}(R, z)}{e^{\frac{-|z|}{h_z(R)}}}, \quad (4)$$

where $h_z(R)$ is taken from eq. (3) for $R < 5.9$ kpc and from L02 for $R > 5.9$ kpc, in order to keep the continuity of h_z. This is represented in Fig. 9. For $R > 5$ kpc the dispersion is larger because the points stem from the counts of very bright red clump sources (which are few in number), so they have significant Poisson noise and also an important contamination of M-giants. It is remarkable how low the dispersion of points is for $R < 4$ kpc and how clearly the density does not increase exponentially towards the centre. If eq. (3), representative of the scaleheight in the inner disc, was greatly in error, the dispersion for $R < 4$ kpc would be much higher, since we have used data with $|b|$ between 2° and 6°.

If we fit a linear relationship in Fig. 9 for $R < 4.25$ kpc, we obtain:

$$\rho_{\mathrm{K2\,III}}(R, 0) = (4.57 \pm 0.33)[1$$

$$- 0.150 \pm 0.033(R(\mathrm{kpc}) - 4)]\rho_{\mathrm{K2\,III},\odot}; \quad (5)$$

for 2.25 kpc < R < 4.25 kpc, where $\rho_{\mathrm{K2\,III},\odot} = 1.31 \times 10^{-5}$ pc^{-3} (L02). This shallow rise is incompatible with

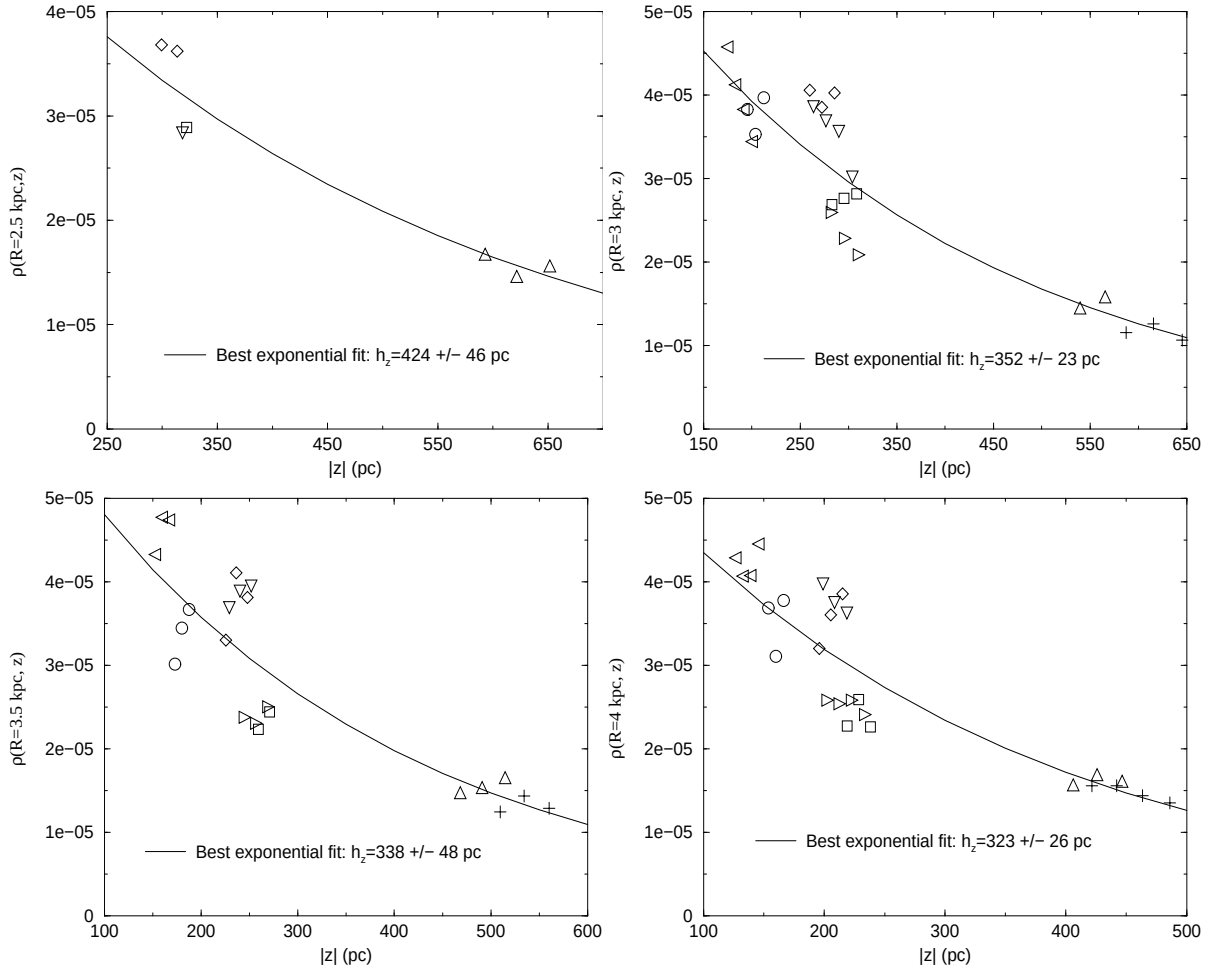

Fig. 8. Density of red clump giants, $\rho_{\rm K2\,III}(R,z)$, at R =2.5, 3.0, 3.5 and 4.0 kpc. The intervals of R are in steps of 0.5 kpc, and the data in each diagram belong to $R-0.25$ kpc $<$ galactocentric radius$<R+0.25$ kpc. Circles: line of sight $l=15°$, $b=2°$; squares: $l=15°$, $b=3°$; diamonds: $l=15°$, $b=-3°$; triangles up: $l=15°$, $b=-6°$; triangles left: $l=18°$, $b=-2°$; triangle down: $l=18°$, $b=-3°$; triangle right: $l=20°$, $b=-3°$; plus: $l=20°$, $b=-6°$. Best exponential fit vs. z is also plotted.

an extrapolation of the outer exponential disc towards the centre. Although the data to 2 kpc show a slight increase of the density towards the centre, a constant density is also consistent within the systematic errors ($\Delta\rho/\rho\sim 20\%$). If we neglect the small gradient with the galactocentric radius in the plane (since the systematic errors are larger than these small variations and we cannot be sure that the gradients are real), then

$$\rho_{\rm K2\,III}(R,z=0)\approx 5.1\rho_{\rm K2\,III,\odot}, \quad (6)$$

for 2.25 kpc $<$ R $<$ 4.25 kpc. We can also fit a more complex law, like a modified exponential (already used for instance by Lépine & Leroy 2000):

$$\rho(R,z=0)=\rho_\odot e^{\left(\frac{R_\odot}{H}+\frac{H_2}{R_\odot}\right)}e^{-\left(\frac{R}{H}+\frac{H_2}{R}\right)}, \quad (7)$$

where $\rho_\odot = 1.31\times10^{-5}$ pc^{-3} and $H=1.97$ kpc are already known from L02, and the parameter H_2 is fitted with our data (see Fig. 9) with a best value of:

$$H_2 = 3740\pm130 \text{ pc}. \quad (8)$$

The fit of eqs (5) and (7), or eq. (6), together with eq. (3), is also applicable away from the plane, as can be observed in Fig. 10. Observe that for lower z, the observed density is lower than the extrapolation of the exponential law, while for higher z the density increases towards the centre more rapidly than the extrapolation of the L02 model. That is, the deficit of stars with respect to the L02 disc affects the regions near the plane. Also, Fig. 7 shows that the present model fits the density obtained directly from the counts (as a function of the distance from the Sun for the different lines of sight).

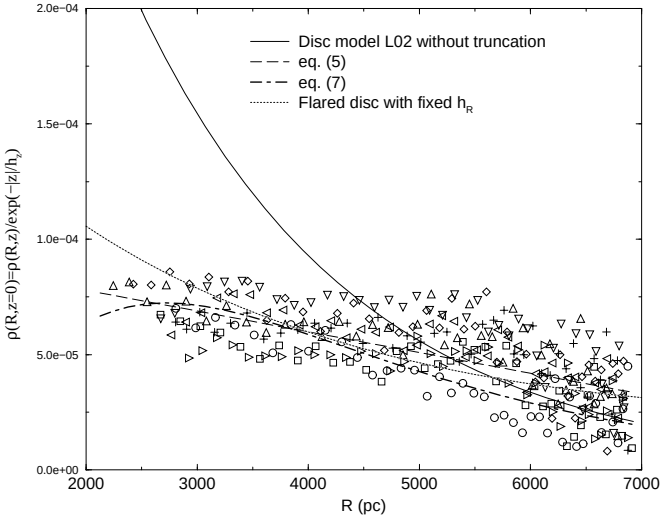

Fig. 9. Density of red clump giants in the plane [derived indirectly from the counts, using the scaleheight $h_z(R)$ from eq. (3) for $R < 5.9$ kpc and from L02 for $R > 5.9$ kpc]. Note that the data for $R > 5$ kpc ($r < 3$ kpc) have large errors due to Poisson noise and M-giant contamination. Exponential disc model taken from an extrapolation of L02 outer disc model. Circles: line of sight $l = 15°$, $b = 2°$; squares: $l = 15°$, $b = 3°$; diamonds: $l = 15°$, $b = -3°$; triangles up: $l = 15°$, $b = -6°$; triangles left: $l = 18°$, $b = -2°$; triangle down: $l = 18°$, $b = -3°$; triangle right: $l = 20°$, $b = -3°$; plus: $l = 20°$, $b = -6°$.

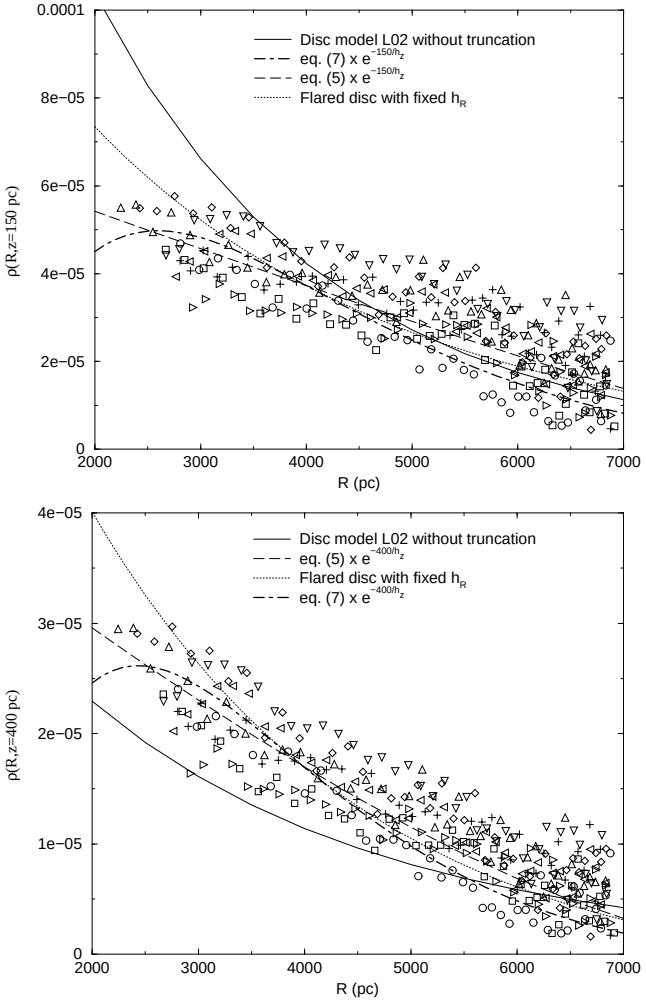

Fig. 10. Density of red clump giants at fixed $z = 150$ pc and 400 pc [derived indirectly from the counts using the scaleheight $h_z(R)$ from eq. (3) for $R < 5.9$ kpc and from L02 for $R > 5.9$ kpc]. Symbols are the same than in Fig. 9.

3.2.1. Flare in the inner disc

Another way to interpret the observed effect is the existence of a flare in the inner disc, which redistributes the stars of the plane in off-plane regions. In L02 we considered an exponential distribution for the density where the flare affects both the scaleheight (which increases with the galactocentric distance) and the flare scalelength (which changes, causing the scalelength of the disc space density, H, to remain constant; see L02 for details). However, the observed effect in the in-plane density at the central Galaxy can also be reproduced by an inner flared disc. If we consider a disc with a fixed exponential scalelength of the disc surface density, and we flare this disc vertically by the flaring law defined in eq. (3), conserving the mass, i.e., the stellar surface density, we find a radial law for the disc density consistent with the observed counts. Considering a fixed scalelength of $h_R = 2.4$ kpc, for example, the agreement is quite good between the observed and predicted densities in the plane in the range 2–8 kpc. As a comparison, in L02 the scalelength of the disc surface density is $h_R = 3.2$ kpc in the outermost disc ($R >$10 kpc), but the flare scalelength changes as the intrinsic scalelength of the disc varies.

In Fig. 9, we represent the predicted densities for four different models: i) the extrapolation of the exponential L02 model, ii) a linear relationship for $R < 4.25$ kpc as given by eq. (5), iii) the modified exponential given by eq. (7) and iv) a flared disc with a fixed scalelength of the surface density (h_R = constant). In each case, except for the extrapolation of the L02 model, there is a good match between the predicted and observed density. This agreement is also observed away from the plane, where models ii), iii), and iv) predict roughly the same star density (Fig. 10).

However, there are basic differences between a vertical flare and a "hole" in the central disc, the latter being considered as a deficit in the stellar density. While the former retains the vertical column density, in star numbers, a hole in the sense defined here will decrease that column density, and will appear to an external observer looking at the Galaxy face on as a real deficit in the stellar distribution of the central regions as compared to the surroundings.

We plan to investigate further the real nature of this feature of the stellar distribution in a subsequent paper. In the rest of this paper, we will refer to this observed feature as a "hole", without prejudging the true origin of

this decrease in the stellar distribution with respect to the exponential prediction.

3.2.2. Calculations with different band widths in the subtraction of red clump giants

The variation in the width of the band to extract the red clumps could alter the results slightly due to the introduction of certain systematic errors. In this subsection, we will examine how large these effects are.

We have already seen (§3.1.1) that the contamination of the giants cannot emulate such a strong deficit of stars. Furthermore, the contamination would increase the counts with respect the number expected in the L02 model (and the normalization of this model was carried out in regions where the contamination is very low) but never decrease them. A more important source of error could be the higher loss of stars for fainter magnitudes due to the spread away from the 0.4 mag width strip, but we have already verified (§3.1.2) that this effect is unimportant (less than 10% according to calculations).

For a further test of the results, we have checked that changing the aperture of the trace (which also changes the contamination of other sources: dwarfs and M giants; see L02, §3) does not significantly change the density obtained for the inner disc. We have derived expressions (3) and (5) for width 0.6 instead of 0.4 used above, with the result:

$$h_z = 282 \pm 9 - [R(\mathrm{kpc}) - 4]48 \pm 15 \text{ pc}; \quad (9)$$

$$\rho_{\mathrm{K2\,III}}(R,0) = (5.55 \pm 0.34)[1$$

$$-0.024 \pm 0.020(R(\mathrm{kpc}) - 4)]\rho_{\mathrm{K2\,III},\odot};$$

$$\text{for 2.25 kpc} < \mathrm{R} < \text{4.25 kpc}, \quad (10)$$

which is compatible with the previous result. If we reduce the width rather than increasing it, for instance, to a 0.3 mag width instead of 0.4 mag, the results are:

$$h_z = 325 \pm 16 - [R(\mathrm{kpc}) - 4]49 \pm 21 \text{ pc}; \quad (11)$$

$$\rho_{\mathrm{K2\,III}}(R,0) = (5.15 \pm 0.40)[1$$

$$-0.165 \pm 0.037(R(\mathrm{kpc}) - 4)]\rho_{\mathrm{K2\,III},\odot};$$

$$\text{for 2.25 kpc} < \mathrm{R} < \text{4.25 kpc}. \quad (12)$$

There are some small differences that can stem from the different degree of contamination from stellar types other than K2 III (a width of 0.6 is more contaminated), and the different degree of patchiness of extinction (this affects the width 0.3 more; see §3.1.2). These small differences do not change any of the conclusions.

On the other hand, the possible errors in the characterization of the K2 III stars would move the position of the beginning of this non-exponential distribution, but never reproduce the shape of $\rho_{\mathrm{K2\,III}}(R, z = 0)$ decreasing towards the centre.

3.2.3. Summary of the results of this section

A rough expression for the central inner disc density is:

$$\rho(R,z) \approx 5.1\rho_\odot e^{\frac{-|z|}{(509-48R(\mathrm{kpc})\ \mathrm{pc})}} \quad (13)$$

This is applicable to 2.25 kpc $< R <$ 4.25 kpc, and the region of transition with the outer L02 disc would be abrupt. A more realistic model is likely to have a smooth transition between 4 and 6 kpc, perhaps something like eq. (19). This expression, eq. (13), is equivalent to:

$$\rho(R,z) \approx \rho_\odot e^{\frac{-(R-R_\odot)}{2.4\ \mathrm{kpc}}} e^{\frac{-|z|}{(509-48R(\mathrm{kpc})\ \mathrm{pc})}} \frac{285 \text{ pc}}{h_z(R)}, \quad (14)$$

a flared disc with a fixed scalelength of 2.4 kpc and a scaleheight that varies according to eq. (3).

Due either to a central hole in the stellar distribution or to a flared disc that redistributes the stars in higher heights above the plane, there is a quite significant deficit of K2 III stars in Galactic plane in the inner disc. Therefore, although we must treat these results with some care, we think that the present conclusions of this section are to be considered as a tentative detection of a flat (rather than exponential) density distribution in the inner disc of our Galaxy for near plane regions. A remarkable aspect of this deficit of stars is that it affects mainly low z, i.e. low-latitude regions, because the larger scaleheight in the central regions compensates for the deficit of star for higher latitudes (see Fig. 10). This agrees with the fact that the deficit was not detected in Baade's windows (at $b = -3.9°$) (Kiraga et al. 1997). High z regions in the model do not have a large deficit of K2 III stars but even an excess with respect to the extrapolation of L02 outer disc model (see Fig. 10 for $z = 400$ pc). Presumably, the deficit of stars affects only the near-plane regions, where the disc material can be swept up due to the motion of the in-plane bar (Athanassoula 1992, L01).

4. Star counts in the near-infrared

A flat density distribution in the inner disc would also produce a deficit of star counts relative to an exponential disc. Counts up to magnitude 9 in the K band are representative of the old stellar population and are appropriate for studying the central regions of the Galaxy. Much deeper counts would make the local disc predominant instead (Garzón et al. 1993).

In Figs 11 and 12 we see how the model with a flat density distribution fits the counts in off-plane regions quite well, while the extrapolation of the L02 external disc model or the B02 disc model (the luminosity function and the extinction were taken from the SKY model; updated version of Wainscoat et al. 1992) is significantly worse, especially for near-plane regions. All models were normalized to give the best fit to the counts presented in Fig. 11. The extinction is very small, so it does not matter whether the applied corrections are totally accurate. No attempt is made to fit the plane ($z = 0$) regions, where

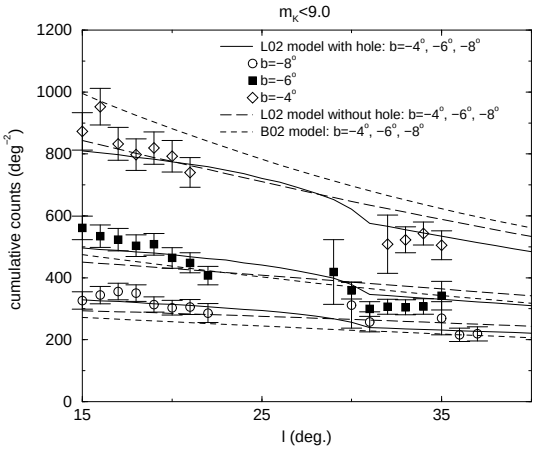

Fig. 11. 2MASS star counts with $m_K \leq 9.0$ for $15° < l < 40°$. Comparison with B02 disc model, and the extrapolation of the L02 model of outer disc towards the centre with exponential and flat density distribution (this paper) are shown. All models were normalized to give the best fit to the counts.

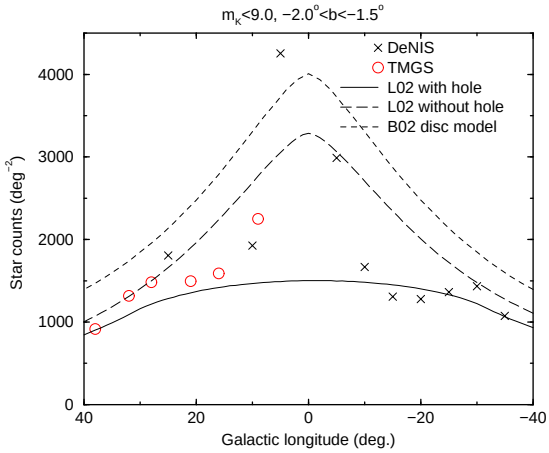

Fig. 12. DENIS/TMGS star counts with $m_K \leq 9.0$ for $-2° < b < -1.5°$ (L01). Comparison with the B02 disc model, and the extrapolation of the L02 model of outer disc towards the centre with an exponential and flat density distribution (this paper) are shown, with the same normalization as in Fig. 11. Note that the models represent only the disc (without the bulge, bar and ring) while the counts do include everything in the line of sight.

the in-plane bar (L01) and the higher extinction make the conclusions about the disc less clear.

Since the L02 model is based in star counts, it represents better than B02 (based on flux maps) the variation of counts with latitude. L02 model also includes the variation of $h_z(R)$ (a flare), making h_z lower towards the centre, improving the fit. However, the L02 extrapolation is insufficient to fit the counts, especially in $b = -1.75°$ and also quite remarkably in $b = -4°$; for higher latitudes there are not so many differences. From here it seems clear that both the flare and the inner truncation are necessary to fit the counts.

Obviously, in Fig. 12 we see a high excess of counts in $|l| < 10°$ which is not reproduced by the disc model because it is caused by the bulge. We see also some excess in positive longitudes with respect to negative longitudes, probably due again to the in-plane bar (L01). The most remarkable fact about the disc in Fig. 12 is, as was said in L01, that the counts are constant between $|l| = 15°$ and $|l| = 30°$ (it is clearer at negative longitudes), and this cannot be fitted with a purely exponential disc in the inner stellar disc. COBE/DIRBE data at 2.2 μm also give a nearly flat light distribution, which at least does not decrease towards the centre, for $15° < |l| < 30°$, $b = 0°$ (Hammersley et al. 1994, Fig. 1); although in $b = 0°$ the imprint of other features such as the in-plane bar or spiral arms also appears.

4.1. Discussion of extinction effects

For the near infrared counts, particularly for $|b| = 1.75°$, where the deficit of counts in the central part is more evident (see Fig. 12), the extinction is not very high, making it rather unlikely that this is a problem of the calculation of the extinction. For instance, at $|l| = 15°$ there is a deficit of 30–45% in the counts with respect to the L02 model without a flat inner density (and even more for the B02 model), which would need an error of 0.3–0.4 mag in extinction in order to be explained in terms of dust. With the model that we have used, the total extinction in the Galactic inner disc at $l = 15°$, $b = 1.75°$ is 0.48 mag (up to a distance from the sun of 7.6 kpc). This is consistent with the estimate of the reddening for the red clump stars in the colour–magnitude diagrams (see §3) at $l = 15°$, $b = 2°$, which gives ≈0.45 mag of total extinction up to that distance (for $b = 1.75°$ it would be ∼0.06 mag larger). Another independent estimate based on Schultheis et al. (1999) gives $A_V \approx 5 - 6$ mag for regions in $b = -1.75°$, $7.5° < l < 17.5°$ (see Fig. 8 in L01), i.e. 0.5–0.6 mag in K, smaller than the ∼0.8–0.9 mag or even more, necessary to produce the observed deficit of stars. A further difficult point, in case we suspected that the extinction is responsible for this distribution of counts, would be to explain the constant star counts in $15° < |l| < 30°$. It is difficult to explain an excess of extinction precisely in a region where we know that there is a hole of gas/dust along the line of sight. The possible extra extinction produced by a ring of gas of radius ∼3–4 kpc would give less extinction for lower $|l|$, because the crossing of the line of sight in the ring is more perpendicular to the ring than tangential; and, moreover, the ring is likely to have a significant contribution only for $|b| < 1°$ (L01). Therefore, we feel that many coincidences that would be difficult to explain would need to take place in order to explain the observed facts in terms of only a problem of extinction calculation.

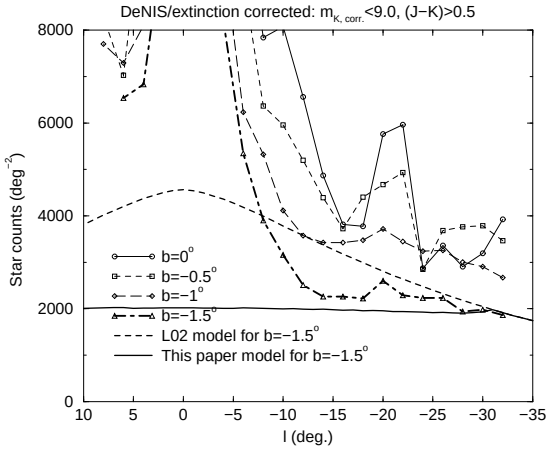

Fig. 13. DENIS star counts with $m_{K,\mathrm{corrected}} \leq 9.0$ and $(J-K) > 0.5$ based on L01-Fig. 10 (see method of extinction correction in L01, using $(J-K)$ colors). $\Delta l = 2°$, $\Delta b = 0.5°$.

Examination of the counts corrected for extinction is a further test that can be carried out. In Fig. 10 of L01, we can see the counts for the negative latitudes after they were approximately corrected for extinction (see L01 for details). The colour $(J-K) > 0.5$ was chosen to remove part of the local disc sources and improve the contrast of distant sources. In Fig. 13 we reproduce the counts of L01 (fig. 10) as a function of longitude for four different latitudes. In this figure, we observe first of all that the stellar 3 kpc arm (that is, the ring, at $l \approx -22°$) affects only those counts for $|b| < 1°$. Second, and more importantly, we can see that the counts are nearly longitude–independent for the range $-32° < l < -16°$ at $b = -1.5°$. This is also true for latitudes closer to the plane, but the 3 kpc arm at $l \approx -22°$ is added. Therefore, we see again that the shape of the counts is incompatible with an exponential disc without truncation, which would give increasing counts towards the centre; in this case, we are talking about counts corrected for extinction. Again, many unlikely coincidences would need to occur to explain the observed facts without the disc truncation.

5. Density distribution of OH/IR stars at 1612 MHz through kinematical distance determination

Stars with high mass-loss rates produce OH masers whose strongest line is at 1612.23 MHz (Elitzur et al. 1976). This allows us to observe these stars at this radio frequency with the advantage of negligible extinction. A complete survey of OH/IR stars in the region $|l| < 45°$, $|b| < 3.25°$, ATCA/VLA OH 1612 MHz, was done by Sevenster et al. (1997a, 1997b, 2001). These sources trace the intermediate–old population when the sources with wind outflow velocity (v_e) less than 14 km s^{-1} are selected, as will be done in this paper; they have an age of $\approx 1.5 - 8$ Gyr (Sevenster 1999). The completeness is very close to 100% for sources with flux larger than 0.375 Jy (Sevenster et al. 1997a); therefore, we use only sources above this limit in this paper.

Star counts cannot be used as a test to discriminate among the models since the number of sources is very small and the Poisson errors dominate. Another direct way to check whether there is a deficit of sources at $R < 4$ kpc is to obtain the distances of the sources. The survey has information on the radial velocities of the sources so, in principle, it is possible to carry out such a test. The only difficulty is that the number of sources is not very high, although high enough to discriminate among the different models. The test is performed as follows: first we calculate the galactocentric distance of each source in certain regions of the sky (which contain inner disc sources but avoiding regions where other components contribute a large number of sources); second, we count the number of sources in the inner disc region in successive radial rings; third, we compare the results with the predictions of different density models using a luminosity function that we also obtain directly from the data.

5.1. Galactocentric distance determination

The first step, the galactocentric distance (R) determination, is carried out through the well known relation between radial velocity, v_r, and R for in-plane regions (Burton 1988, eq. 7.4), assuming circular orbits:

$$v_r = R_\odot \left[\frac{V(R)}{R} - \frac{V(R_\odot)}{R_\odot} \right] \sin l, \tag{15}$$

where $V(R)$ is the rotation velocity of the disc at galactocentric distance R. If we take $V(R) = V(R_\odot)(R/R_\odot)^{0.1}$ km s^{-1} (Binney et al. 1991), this leads to

$$R = \frac{R_\odot}{\left(1 + \frac{v_r}{V(R_\odot)\sin l}\right)^{1.11}}. \tag{16}$$

This equation is applicable because the disc OH/IR stars in the plane follow the galactic rotation (Baud et al. 1981). We adopt $V(R_\odot) = 200$ km s^{-1} (Honma & Sofue 1996) (a value of 220 km s^{-1} would not change the conclusions of this section, but would slightly reduce the values in Fig. 16/Table 2) and $R_\odot = 7.9$ kpc (López-Corredoira et al. 2000). The random motions in the old population are around 30–40 km s^{-1} (Baud et al. 1981). $\sigma_{v_r} \approx 35$ km s^{-1} leads to an error of

$$\sigma_R \approx \frac{0.020}{\sin l} R(\mathrm{kpc})^{1.9} \text{ kpc}, \tag{17}$$

and this leads to important errors only for large values of R and low l. Moreover, the errors for the individual sources are mostly reduced when the statistical count is carried out, except perhaps for the very few sources close to the Sun (high R). In any case, we will include the calculation of this error in this paper to show that even with this error (and the Poisson errors) models with a purely exponential disc are excluded.

5.2. Luminosity function

The previous relation allows us to determine R, but not the distance from the Sun (r) because of the well-known ambiguity of there being two possible values for a given R inside the solar circle (Burton 1988). Therefore, we cannot use this relation to obtain the luminosity function directly.

To estimate the luminosity function, we take separately the sources in the centre of the Galaxy ($|l| < 3^\circ$, $|b| < 3^\circ$) and assume that all of them are at the same distance ($R_0 = 7.9$ kpc). The contribution of foreground disc sources is small. To reduce this disc contamination further, we take the sources with radial velocities $|v_r| > 30$ km s^{-1}, since the disc sources in this direction are expected to have near-zero radial velocities. Fig. 14 shows the cumulative luminosity distribution of this subsample (luminosity in units Jy kpc^2, i.e. the flux of the source in Jy considering the source located at a distance of 1 kpc) which can be fitted by:

$$\int_{L_0}^{\infty} \phi(L) dL \propto L_0^{-1.20}, \quad (18)$$

that is, a luminosity function $\phi(L) \propto L^{-2.20}$. This relation is fitted for $L_0 > 0.375 R_\odot(\mathrm{kpc})^2$ Jy kpc^2, the detection limit. The exponent, $\alpha = -2.2$, is close to the value of -2.0 obtained also in the Galactic center by Herman & Habing (1985). Chengalur et al. (1993) obtained a value of -1.5 and Baud et al. (1981) obtained a value of -1.65, but their samples also contained young population (high v_e), so the difference could stem from this. We are interested here only in the old population (older than 1.5 Gyr). A power law is generally accepted as a fit to the luminosity function, at least in the observed range.

There is a cut-off for the faintest luminosities (Baud et al. 1981), which we take to be at $L_0 < 0.2 R_\odot(\mathrm{kpc})^2$ Jy kpc^2, since the luminosity function peaks around $L_0 = 0.2 R_\odot(\mathrm{kpc})^2$ Jy kpc^2 (Sjouwerman et al. 1998), and the number of fainter sources is lower (so the factor r^2 will make the number of nearby faint sources negligible). Debattista et al. (2002) have also verified that the number of low luminosity sources is very small (corresponding to low v_e; luminosity is correlated with v_e but the relation between both parameters cannot be used as a distance indicator since the dispersion of luminosities for a given v_e is large). Fig. 9 in Debattista et al. (2002) shows that there are practically no low-luminosity stars ($v_e < 6$ km s^{-1}; roughly less than $0.2 R_\odot(\mathrm{kpc})^2$ Jy kpc^2 in average) at $20^\circ < |l| < 45^\circ$ in the ATCA/VLA survey. Also, Sevenster et al. (1997a, fig. 6b; 2001, fig. 5b) find a very low number of low-v_e sources in the whole survey.

With the luminosity function and the densities of the L02 or B02 models, we can calculate the number of counts in a given region of the sky as a function of R, and compare them with the distribution obtained from the data through eq. (16). Fig. 15 shows the result for $R > 4$ kpc in $12.8^\circ < |l| < 45^\circ$. This figure shows an agreement between models and data at $R > 4$ kpc which corroborates that the luminosity function is approximately correct.

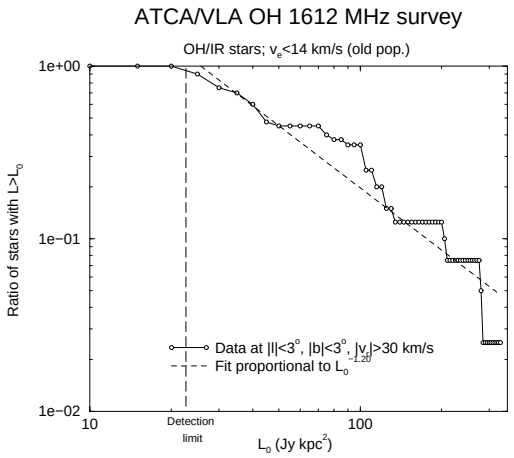

Fig. 14. Luminosity distribution of ATCA/VLA-1612 MHz survey sources in the centre of the Galaxy ($|l| < 3^\circ$,$|b| < 3^\circ$) and with radial velocities $|v_r| > 30$ km s^{-1}.

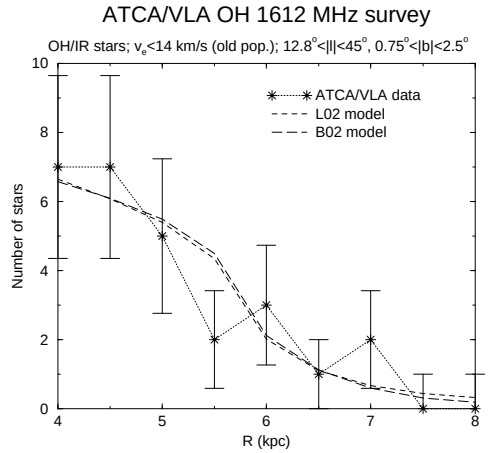

Fig. 15. Distribution of ATCA/VLA-1612 MHz survey sources (flux larger than 0.375 Jy, outflow velocities $v_e <$ 14 km s^{-1}) in the region $12.8^\circ < |l| < 45^\circ$, $0.75^\circ < |b| < 2.5^\circ$ as a function of the galactocentric radii for $R > 4$ kpc. Model normalized to give the same number of sources than the data. Error bars stand only for Poisson errors. There is a good agreement with the B02 or L02 models (it does not matter whether it has a flat distribution or not, since this does not affect the regions at $R > 4$ kpc) in this range of R.

5.3. Deficit of stars in the inner disc

If we apply this technique to the inner disc regions, we can see whether the model of §3 does or does not fit better than the L02 or B02 exponential models. We select the region $|l| > 12.8^\circ$ (i.e. $R > 1.75$ kpc), $0.75^\circ < |b| < 2.5^\circ$ because this is far enough away from the bulge; it crosses the inner disc and is far enough away from the plane to consider the contribution of other possible plane old-population components (bar, ring) small in comparison to the error bars of the data. Rather than a plot as a

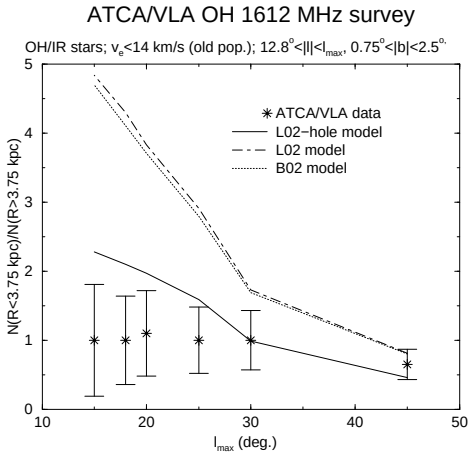

Fig. 16. Distribution of ATCA/VLA-1612 MHz survey sources (flux greater than 0.375 Jy, outflow velocities $v_e < 14$ km s^{-1}) in the region $12.8^\circ < |l| < l_{\max}$, $0.75^\circ < |b| < 2.5^\circ$. Note that the points are not independent, however the point at $l_{\max} = 18^\circ$ is enough to reject the B02 and L02 models beyond the 5σ level.

function of R (as in Fig. 15), we will show the ratio between lower and higher R sources, between the sources in the inner disc ($R < 3.75$ kpc) and the remainder. The Poisson errors are very large if we divide the data into bins with different R. By means of eq. (16), the ratio $\left(\frac{N(R<3.75\ \mathrm{kpc})}{N(R>3.75\ \mathrm{kpc})}\right) = \left(\frac{N([v_r/\sin l]>190\ \mathrm{km/s})}{N([v_r/\sin l]<190\ \mathrm{km/s})}\right)$ is shown in Table 2. The lower the maximum longitude, the more sensitive we are to the inner disc population; however, the Poisson errors are larger (because we have fewer sources). Restricted to $|l| < 18^\circ$, we get the larger discrepancy: the differences of an exponential model and the results from the data are around 5σ, significant enough. Figure 16 shows this graphically.

The model of this paper gives a much better fit: all the ranges in Table 2 are within the 1.8σ level. Perhaps the deficit of stars should be larger than that calculated in §3, but since we have not taken into account the errors of eq. (13) and the interpolation of the transition region, the compatibility with the flat distribution described in this paper is not excluded.

Therefore, the conclusion of this section is again that a deficit of stars is necessary in the old population (older than 1.5 Gyr) of the disc with a density amplitude similar to that derived in §3, or even lower. It is noteworthy that this deficit of old population OH/IR stars has already been argued by Baud et al. (1981) for the populations around 1 Gyr old. We quote a paragraph from §6.4 of this paper[1]:

> That the sources with large ΔV exhibit the same kind of overall density distribution is to be expected when they are as young as we have estimated. But the similarity of the density distribution of the sources with small $\Delta V (\approx 10^9$ yr old) and the extreme Population I objects is surprising. We interpret this to mean that the large-scale CO distribution in the disc and hence the region of active star formation has not changed significantly during the last 10^9 yr, or 4-8 rotations of the Galaxy. Therefore the 'hole' in the gas and in the OH/IR sources distribution at $R < 4.5$ kpc and the maximum density at $R = 5$ kpc appear to be rather stable phenomena.

We corroborate these words for even older stars.

[1] Baud et al. call the separation between the two peaks of OH/IR sources at 1612 MHz $\Delta V = 2v_e$ and use $R_\odot = 10$ kpc.

6. Counts with bright sources in the mid-infrared

In this section, we compare the disc models with bright mid-infrared star counts in the plane (i.e. a young population). In the mid-infrared, there is practically zero extinction (∼70 smaller than in V) even in plane regions. This means that extinction in the plane (b=0°) is typically 0.1–0.2 mag in the mid-infrared, except in the very centre, where it can reach 0.4 mag.

The comparison is carried out in Fig. 17. In this case, MSX counts at 14.6 μm up to magnitude 3.0 are compared with different models. This is compared with the B02 model prediction (the luminosity function and the extinction were taken from the SKY model; updated version of Wainscoat et al. 1992) and with the extrapolation of the outer disc according to L02. Obviously, the L02 and B02 models fail to reproduce the data for $|l| < 30^\circ$. COBE/DIRBE data at 12 μm, representative of the flux of the young population, also give a nearly flat light distribution at $10^\circ < |l| < 30^\circ$, $b = 0^\circ$ (Hammersley et al. 1994, fig. 1) instead of increasing towards $l = 0^\circ$. Comparison with the models shows that the inner truncation of the exponential increase in the density in the disc can explain the difference. The model of this paper, which follows eq. (13) for $R < 4$ kpc, can roughly fit the counts. Errors in the extinction are very low and cannot explain the observed difference between data and exponential models. The bulge, spiral arms, ring and in-plane bar also have some contribution which is not calculated here; note, however, that they would increase the number of counts but never decrease it, so the interpretation of a deficit of stars is unavoidable. No attempt is made to fit the counts for other latitudes because we would need the scaleheight and the flare of the observed population with MSX-14.65 μm, dominated by a young population, and this is at present unknown.

7. Summary of results: a smooth model for outer and inner disc

We have used three different methods: 1) the inversion of the red clump giant distribution in near-infrared colour–magnitude diagrams to obtain the star density along the line of sight; 2) the determination of the density distribution of 1612 MHz sources by means of the distance

Table 2. The $\left(\frac{N(R<3.75\ \mathrm{kpc})}{N(R>3.75\ \mathrm{kpc})}\right)$ ratio in the ATCA/VLA 1612 MHz survey and the predictions of three different models. Range of latitudes: $0.75^\circ < |b| < 2.5^\circ$. Errors in the data include Poisson errors and the errors due to the dispersion of values in R calculated according to eq. (17) [estimated by means of a Monte Carlo simulation].

Long. range	Data	Model "This paper"	Model L02	Model B02
$12.8^\circ < \|l\| < 45^\circ$	0.65±0.22	0.46	0.81	0.80
$12.8^\circ < \|l\| < 30^\circ$	1.00±0.43	0.99	1.73	1.69
$12.8^\circ < \|l\| < 25^\circ$	1.00±0.48	1.59	2.91	2.79
$12.8^\circ < \|l\| < 20^\circ$	1.10±0.62	1.97	3.83	3.71
$12.8^\circ < \|l\| < 18^\circ$	1.00±0.64	2.10	4.30	4.11
$12.8^\circ < \|l\| < 15^\circ$	1.00±0.81	2.28	4.84	4.70

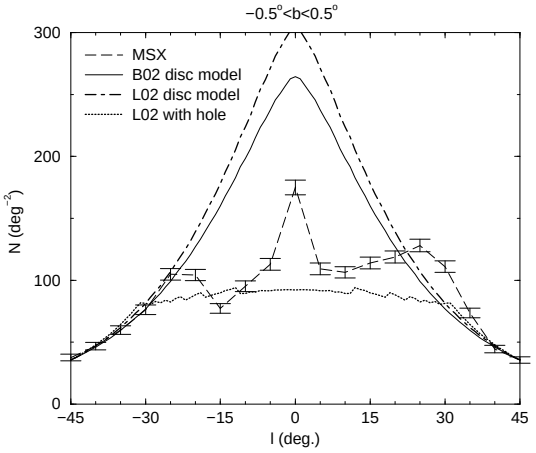

Fig. 17. MSX star counts in the plane at 14.6 μm up to magnitude 3.0. Comparison with the B02 disc model and the extrapolation of the L02 model of outer disc towards the centre with an exponential and flat density distribution (this paper). All models were normalized with the counts to fit the counts at $l = 45^\circ$. It is clear that the deficit of stars in the young stellar population represented here is necessary. Note that the models represent only the disc (without a bulge, bar or ring) while the counts include everything in the line of sight.

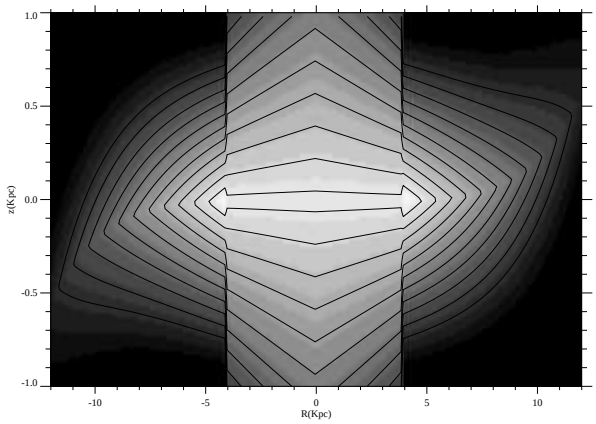

Fig. 18. Contour diagram of $\log_{10}\rho\ (\mathrm{pc}^{-3})$ in the yz-plane of the Galaxy (perpendicular to the line Sun–Galactic centre) with y between -12.0 and 12.0 kpc and z between -1.0 and 1.0 kpc (vertical scale in the plot multiplied by a factor 5). Lower contour: $\log_{10}\rho\ (\mathrm{pc}^{-3})$=-2.1; step=0.15. Model: L02 for $R > 4$ kpc, and eq. (13) for $R \leq 4$ kpc. The abrupt transition (at $|y| = R = 4$ kpc) is due to the discontinuous change of regime between the inner disc and the outer disc. Note also that the model of this paper is valid only for regions not very far from the plane.

determination of OH/IR sources from their kinematical information; 3) the analysis of near-infrared star counts and comparison with models. All the tests agree with the following picture for the inner disc:

- There is a deficit of stars with respect to an exponential disc in the Milky Way's inner stellar disc for 2.25 kpc $< R <$ 4 kpc. The density in the plane ($b \approx 0^\circ$, i.e. $z \approx 0$) is almost independent of R instead of being an exponential law of the type $\rho \propto \exp(-R/h)$.
- There is a slight increase in scaleheight in the central disc, $h_z = 509 - 48R(\mathrm{kpc})$ pc, so the combined effect of deficit of stars in the plane and higher scaleheight produces an important deficit of stars for low latitude regions, although not for high latitude regions. Roughly, the density follows an expression of the type $\rho(R,z) \approx 5.1 \pm 0.6\rho_\odot e^{\frac{-|z|}{509\pm67-48\pm20R(kpc)\ \mathrm{pc}}}$, a result that is also compatible with a flared inner disc with a fixed scalelength of 2.4 kpc: $\rho(R,z) \approx \rho_\odot e^{\frac{-(R-R_\odot)}{2.4\mathrm{kpc}}} e^{\frac{-|z|}{509\pm67-48\pm20R(kpc)\ \mathrm{pc}}} \frac{285\ \mathrm{pc}}{509\pm67-48\pm20R(kpc)\ \mathrm{pc}}$.

It is our objective to investigate further the real nature of the inner stellar disc, with a more complete analysis of 2MASS *All Sky Release* star counts. See the graphical representation in Fig. 18 (both possibilities are numerically equivalent). Note that these numbers are also subject to several systematic errors ($\lesssim 15\%$ in the density between latitudes 2 and 6 degrees), so the parameters might change; although not as much as to allow the fit of a purely exponential disc (which would require errors greater than 70%). Moreover, the deficit of stars is corroborated with the OH/IR sources and the star counts. These parameters are applicable only for regions not very far from the plane ($|b| < 6^\circ$).

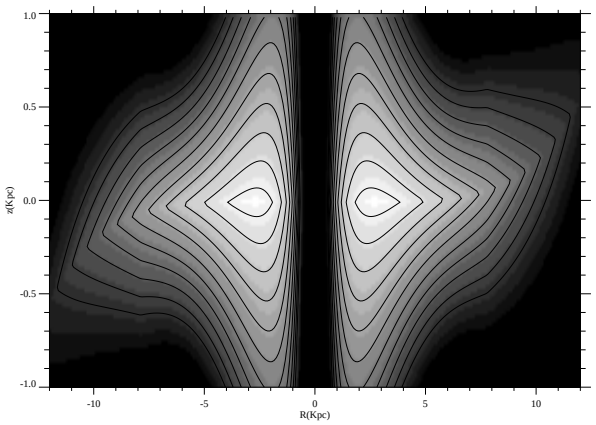

Fig. 19. Contour diagram of $\log_{10}\rho$ (pc^{-3}) of a possible interpolated/extrapolated smooth model of the disc according to eq. (19) for $R < R_\odot$ and L02 for $R \geq R_\odot$ in the yz-plane of the Galaxy (perpendicular to the line Sun–Galactic Centre) with y between -12.0 and 12.0 kpc and z between -1.0 and 1.0 kpc (vertical scale in the plot multiplied by a factor 5). Lower contour: $\log_{10}\rho$ (pc^{-3}) $= -2.1$; step $= 0.15$.

– Both the young and old population have this deficit of stars, and at present no significant differences in their distributions have been deduced from the data. Presumably, a more accurate measure of the distribution might reveal some differences. At present we can say that, roughly speaking, the deficit of stars with respect the extrapolation of an exponential distribution is probably a rather stable feature of the disc, which might be due to the existence of an in-plane bar that sweeps out the near-plane stars.
– An expression that summarizes the L02 outer disc ($R > 6$ kpc) and the inner disc (2.5 kpc $< R <$ 4 kpc) with a smooth transition between two regimes is:

$$\rho(R,z) \approx \left[\rho_\odot e^{\left(\frac{R_\odot}{1970\ pc}+\frac{3740\ pc}{R_\odot}\right)}\right] \times e^{-\left(\frac{R}{1970\ pc}+\frac{3740\ pc}{R}\right)} e^{-|z|/h_z}, \quad (19)$$

with

$$h_z(R) \approx 285[1 + 0.21\ \mathrm{kpc}^{-1}(R-R_\odot) + 0.056\ \mathrm{kpc}^{-2}(R-R_\odot)^2]\ \mathrm{pc}. \quad (20)$$

This density is plotted in Fig. 19. Although this expression was not tested for all ranges (for instance, it is not tested around $R = 5$ kpc or for $R < 2$ kpc), this can be used as an approximate interpolation/extrapolation that models the disc in $R < R_\odot$. For the outermost disc, it is better still to use the expression of L02. The innermost disc ($R < 2$ kpc) reveals with the expression (19) a very deep hole. Unfortunately, we cannot be sure of the existence of this deep hole there, since the disc and the bulge cannot be easily separated in that region. It is clear at least that between 2 and 4 kpc the deficit of stars is very significant.

Acknowledgments: We thank C. Alard, V. P. Debattista and P. L. Hammersley. This publication makes use of data products from 2MASS (which is a joint project of the Univ. of Massachusetts and the Infrared Processing and Analysis Center (IPAC), funded by the NASA and the NSF); the MSX Point Source Catalog (which was obtained from the NASA/IPAC Infrared Science Archive at Pasadena, California); DENIS (the result of a joint effort involving personnel and financial contributions from several Institutes, mostly located in Europe and supported financially mainly by the French Institute National des Sciences de l'Univers, CNRS, and French Education Ministry, the European Southern Observatory, the State of Baden-Württemberg, and the European Commission under a network of the Human Capital and Mobility programme), the TMGS (based on observations made at Carlos Sánchez Telescope operated by IAC at Teide Observatory on the island of Tenerife), the ATCA/VLA OH 1612-MHz survey (based on observations made by Sevenster et al. at the Australia Telescope Compact Array and at the Very Large Array).

References

Aguerri, J. A. L., Hunter, J. H., Prieto, M., et al. 2001, A&A, 373, 786
Alard, C. 2000, astro-ph/0007013
Anderson, K. S. J., Baggett, S. M., & Baggett, W. E. 2002, AAS, 200, 4313
Athanassoula, E. 1992, MNRAS, 259, 345
Baggett, W. E., Baggett, S. M., & Anderson, K. S. J. 1998, AJ, 116, 1626
Baud, B., Habing, H. J., Matthews, H. E., & Winnberg, A. 1981, A&A, 95, 156
Binney, J. J., Gerhard, O. E., Stark, A. A., Bally, J., & Uchida, K. I., 1991, MNRAS, 252, 210
Bissantz, N., & Gerhard, O. E. 2002, MNRAS, 330, 591 (B02)
Bottema, R., & Verheijen. M. A. W. 2002, A&A, 388, 793
Burton, W. B. 1988, in: Galactic and Extragalactic Radio Astronomy, eds., G. L. Verschuur, K. I. Kellerman (Springer Verlag, Berlin), p. 295
Burton, W. B. & Te Lintel Hekkert, P. 1986, A&AS, 65, 427
Caldwell, J. A. R., & Ostriker, J. P. 1981, ApJ, 251, 61
Cohen, M., Hammersley, P.L., & Egan, M.P. 2000, AJ, 120, 3362
Chengalur, J. N., Lewis, B. M., Eder, J., & Terzian, Y. 1993, ApJS, 89, 189
Debattista, V. P., Gerhard, O., & Sevenster, M. N. 2002, MNRAS, 334, 355
Egan, M. P. et al., 1999, "The Midcourse Space Experiment Point Source Catalog Version 1.2 Explanatory Guide", Air Force Research Laboratory Technical Report, AFRL-VSTR 1999-1522
Elitzur, M., Goldreich, P., & Scoville, N. 1976, ApJ, 205, 384
Freeman K. C. 1970, ApJ, 160, 811
Freudenreich H. T., 1998, ApJ, 492, 495

Garzón, F., Hammersley, P. L., Mahoney, T., et al. 1993, MNRAS, 264, 773
Grocholski A. J., & Sarajedini A. 2002, AJ, 123, 1603
Hammersley, P. L., Garzón, F., Mahoney, T., & Calbet, X. 1994, MNRAS, 269, 753
Hammersley, P. L., Garzón, F., Mahoney, T., López-Corredoira, M., & Torres, M.A.P. 2000, MNRAS, 317, L45
Herman, J., & Habing, H. J. 1985, Phys. Rep., 124(4), 255
Honma, M., & Sofue, Y. 1996, PASJ, 48, L103
Kiraga, M., & Paczyński, B. 1994, ApJ, 430, L101
Kiraga, M., Paczyński, B., & Stanek, K. Z. 1997, ApJ, 485, 611
Lada, C. J., Alves, J., & Lada, E. A. 1999, ApJ, 512, 250
Lépine, J. R. D., & Leroy, P. 2000, MNRAS, 313, 263
López-Corredoira, M., Hammersley, P. L., Garzón, F., Simonneau, E., & Mahoney, T. J. 2000, MNRAS, 313, 392
López-Corredoira, M., Hammersley, P. L., Garzón, F., et al. 2001, A&A, 373, 139 (L01)
López-Corredoira, M., Cabrera-Lavers, A., Garzón, F., & Hammersley, P. L. 2002, A&A, 394, 883 (L02)
Nikolaev, S., Drake, A. J., Keller, S. C., Cook, K. H., Dalal, N., Griest, K., Welch, D. L., & Kanbur, S. M. 2004, ApJ, 601, 260
Ohta, K., Hamabe, M., & Wakamatsu, K. 1990, ApJ, 357, 71
Pietrzyński, G., Gieren, W.,& Udalski, A. 2003, AJ, 125, 2494
Rieke, G. H., & Lebovsky, M. J. 1985, ApJ, 288, 618
Robinson, B. J., Manchester, R. N., Whiteoak, J. B., Otrupcek, R. E., & McCutcheon, W. H. 1988, A&A, 193, 60
Sakamoto, K., Okumura, S. K., Ishizuki, S., & Scoville, N. Z. 1999, ApJS, 124, 403
Salaris, M., & Girardi, L. 2002, MNRAS, 337, 332
Sancisi. R. 1999, Ap&SS, 269, 59
Schultheis, M., Ganesh, S., Simon, G., et al. 1999, A&A, 349, L69
Sevenster, M. N. 1999, MNRAS, 310, 629
Sevenster, M. N., Chapman, J. M., Habing, H. J., Killeen, N. E. B., & Lindqvist, M. 1997a, A&AS, 122, 79
Sevenster, M. N., Chapman, J. M., Habing, H. J., Killeen, N. E. B., & Lindqvist, M. 1997b, A&AS, 124, 509
Sevenster, M. N., van Langevelde, H., Chapman, J. M., Habing, H. J., & Killeen, N. E. B. 2001, A&A, 366, 481
Sjouwerman, L. O., van Langevelde, H. J., Winnberg, A., & Habing, H. J. 1998, A&AS, 128, 35
Skrutskie M. F., Schneider S. E., Stiening R., et al. 1997, in: The Impact of Large Scale Near-IR Sky Surveys, F. Garzón F., N. Epchtein N., A. Omont, B. Burton, P. Persi, eds., Kluwer, Dordrecht, p. 25
Wainscoat, R. J., Cohen, M., Volk, K., Walzer, H. J., & Schwartz D. E. 1992, ApJS, 83, 111